J. Membrane Biol. 28, 41 – 70 (1976)

The Mechanism of Na^+ Transport by Rabbit Urinary Bladder

Simon A. Lewis*, Douglas C. Eaton*, and Jared M. Diamond

Physiology Department, University of California Medical Center, Los Angeles, California 90024

Received 21 October 1975; revised 3 February 1976

Summary. The mechanism of Na^+ transport in rabbit urinary bladder has been studied by microelectrode techniques. Of the three layers of epithelium, the apical layer contains virtually all the transepithelial resistance. There is radial cell-to-cell coupling within this layer, but there is no detectable transverse coupling between layers. Cell coupling is apparently interrupted by intracellular injection of depolarizing current. The cell interiors are electrically negative to the bathing solutions, but the apical membrane of the apical layer depolarizes with increasing I_{sc}. Voltage scanning detects no current sinks at the cell junctions or elsewhere. The voltage-divider ratio, α, (ratio of resistance of apical cell membrane, R_a, to basolateral cell membrane, R_b) decreases from 30 to 0.5 with increasing I_{sc}, because of the transport-related conductance pathway in the apical membrane. Changes in effective transepithelial capacitance with I_{sc} are predicted and possibly observed. The transepithelial resistance, R_t, has been resolved into R_a, R_b, and the junctional resistance, R_j, by four different methods: cable analysis, resistance of uncoupled cells, measurements of pairs of (R_t, α) values in the same bladder at different transport rates, and the relation between R_t and I_{sc} and between α and I_{sc}. R_j proves to be effectively infinite (nominally 300 kΩ μF) and independent of I_{sc}, and R_a decreases from 154 to 4 kΩ μF with increasing I_{sc}. In the resulting model of Na^+ transport in "tight" epithelia, the apical membrane contains an amiloride-inhibited and Ca^{++}-inhibited conductance pathway for Na^+ entry; the basolateral membrane contains a $Na^+ - K^+$-activated ATPase that extrudes Na^+; intracellular (Na^+) may exert negative feedback on apical membrane conductance; and aldosterone acts to stimulate Na^+ entry at the apical membrane via the amiloride-sensitive pathway.

In the previous paper (Lewis & Diamond, 1976) we demonstrated that rabbit urinary bladder actively absorbs Na^+, possesses a transport-linked conductance pathway for Na^+, and has a very high electrical resistance when this pathway is inhibited. The close similarities between this preparation and other "tight epithelia", such as frog skin and toad urinary bladder, or between this preparation and "medium-tight epithelia" such as distal tubule and rabbit descending colon, suggest that it may offer a good model

* *Present address:* University of Texas Medical Branch, Department of Physiology and Biophysics, Galveston, Texas 77550.

system for understanding the Na^+ transport mechanism common to these tissues.

In the present paper we use microelectrode techniques to localize elements of the transport system. We seek to answer the following questions:

1. Are the so-called tight junctions really tight? I.e., what are the relative resistances of the cellular and junctional pathways to permeating ions?

2. How is transepithelial resistance apportioned among the three cell layers, and between the apical and basolateral cell membranes of these layers?

3. Which of the three layers of epithelial cells has the pump?

4. Which cell membrane or membranes has the transport-linked conductance pathway?

Materials and Methods

Rabbit urinary bladder was dissected and mounted as described previously (Lewis & Diamond, 1976). Fig. 1 shows the design of the microelectrode chamber. This design had the disadvantage that it permitted some edge damage to develop, as gauged by the fact that transepithelial resistance (5,000–25,000 Ω μF) was somewhat lower than with the chamber design described in the preceding paper (Fig. 1 of Lewis & Diamond, 1976: $R \sim 7{,}000$–$78{,}000$ Ω μF). A Wild dissecting microscope at 100× magnification was used to observe the tissue and the microelectrode shaft with transillumination. The bladder was always mounted with the apical surface up, and microelectrode impalements were always made from this side. Bathing solution temperature was maintained at 37 °C.

Transepithelial resistance R_t, short-circuit current I_{sc}, spontaneous transepithelial voltage V_{sp}, and effective transepithelial capacitance C_t were measured as in the previous paper. Microelectrodes were prepared by a two-stage puller and were selected to have tip resistances in the range $8–20 \times 10^6$ Ω. W. P. Instruments M4A electrometers with internal bridge circuitry were used to measure intracellular voltages and to pass intracellular currents. The mucosal solution was generally grounded.

Cable analysis of radial current spread in the plane of the epithelium was based on experiments with two microelectrodes. One electrode passed 1-sec current pulses between a cell arbitrarily termed the origin cell and either the mucosal or serosal solutions. The magnitude of the current was adjusted so as to give a voltage response of either 6 or 60 mV in the origin cell. Only hyperpolarizing pulses were used, because depolarizing pulses uncouple cells (pp. 13–17). A second microelectrode impaled other cells and thereby mapped the radial potential field around the origin cell. The distance between the two microelectrodes was measured by a calibrated graticule in the microscope eye-piece. The bladder was mounted under moderate stretch so that epithelial folding would not cause the distance measurements to be underestimates. At each successful impalement we applied a transepithelial current pulse and measured either the voltage between the basolateral cell membrane and the serosal solution, or else the voltage between the apical cell membrane and the mucosal solution. We also measured the voltage across the whole epithelium at each impalement. From these measurements the value of basolateral membrane resistance R_b, apical membrane resistance R_a, and junctional resistance R_j may be calculated (*see* assumed equivalent circuit of Fig. 2).

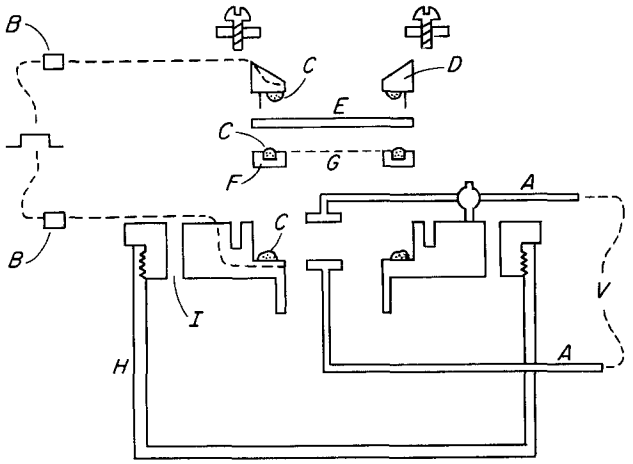

Fig. 1. Design of chamber for microelectrode experiments. *A*, sintered AgCl potential-measuring pellets for recording transepithelial voltage. The pellet in the mucosal solution (above) was mounted on a Teflon gimbel so as not to interfere with the microelectrode. *B*, Ag−AgCl electrodes used to pass transepithelial current. *C*, sealant ring of silicone grease. *D*, upper ring of chamber with 16 pins set into circumference. *E*, bladder. *F*, lower ring of chamber with receptacles for pins. *G*, nylon mesh to support bladder. *H*, lower body of chamber. *I*, port for changing and aerating solutions. The assembly with the tissue, *D-E-F-G*, actually rests between the electrodes *A*

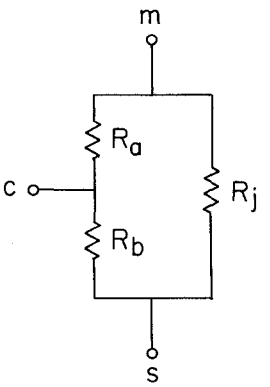

Fig. 2. Simplified circuit diagram of rabbit urinary bladder, with resistors corresponding to cell junctions (R_j) and to apical (R_a) and basolateral cell membranes (R_b) of apical cell layer. The apical layer actually consists of many such circuits in parallel, connected by coupling resistors. The middle and basal cell layers are ignored because of their negligible transepithelial resistance. Symbols *m*, *s* and *c* stand, respectively, for the mucosal solution, serosal solution and cell interior of the apical layer. In practice, V_{cm} or V_{sc} is the potential difference between the mucosal or serosal solution and the cell, where the cell is defined as the first of the three negative potential wells encountered on advancing a microelectrode from the mucosal to the serosal solution. Operationally, R_j includes the effects of edge-damage conductance. Total transepithelial resistance R_t equals $R_j(R_a+R_b)/(R_a+R_b+R_j)$. The so-called voltage divider ratio α is defined as R_a/R_b

These quantities are related to transepithelial resistance R_t by the equation

$$(1/R_t)=(1/R_j)+1/(R_a+R_b). \quad (1)$$

To identify low-resistance current pathways associated with cell junctions or damaged areas or edges by "voltage scanning" (*see* Frömter & Diamond, 1972; and Frömter, 1972 for detailed description), we monitored the voltage differentially between a remote microelectrode in the mucosal solution and a scanning microelectrode (with the tip broken) pulled gently over the apical surface, while passing a square transepithelial current pulse at 1 sec.

To obtain the current-voltage relation of the epithelial cell membranes, a Tektronix 503 series function generator was used to develop a current ramp (an applied current increasing linearly with time) for intracellular injection through a microelectrode. The injected current and the cellular voltage response were recorded on a Hewlett Packard 7004 X-Y recorder. The current-injecting electrode served to record the voltage response. The current-voltage relation of the electrode in free solution was subtracted from its relation when inside a cell to obtain the cell response.

The bathing solutions were (in mM): 110 NaCl, 25 $NaHCO_3$, 7 KCl, 2 $CaCl_2$, 1.2 $MgSO_4$, 1.2 NaH_2PO_4, and 11.1 glucose, buffered at pH 7.4 and gassed with 95% O_2–5% CO_2. In experiments calling for inhibition of I_{sc}, we added microliter quantities of a 1 mM amiloride solution to the mucosal solution.

Results

Criteria for Successful Impalement

The large size of rabbit bladder cells (30 μ in diameter, 20 μ high) made it relatively easy to impale them with microelectrodes and obtain stable recordings. We adopted the following criteria of success: (1) When the apical cell membrane is impaled, the potential must achieve a steady-state value in less than 1 sec. (2) This value must remain stable for the duration of the measurements in this cell. (Generally the value remained stable for up to 15 min). (3) The so-called voltage-divider ratio R_a/R_b must be stable with time. (4) The electrode resistance must be the same before and after impalement, and the measured resistance between the electrode and bathing solution must be higher with the electrode in the cell than in the solution. Figs. 3 and 5 will summarize the result of every impalement that met these four criteria. In practice, no impalement that met these criteria yielded an R_a/R_b value less than 0.5 [*see* Fig. 5, which depicts $G_a/G_b=1/(R_a/R_b)$], and we may therefore conclude that the microelectrode did not introduce a significant leak into the apical membrane in successful impalements.

The average resting potential across the apical cell membrane of the apical cell layer (V_{cm} in Fig. 2) under open-circuit conditions was -25 ± 0.9 mV ($n=98$; this and all other errors to be reported are standard errors of the mean); i.e., cell interior negative to the mucosal solution. Variation in this resting potential among bladders was correlated with

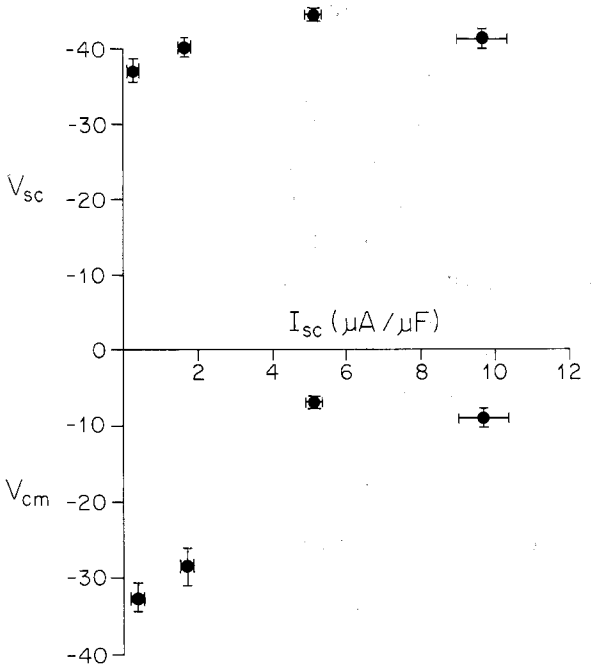

Fig. 3. Cell resting potential (ordinate) as a function of I_{sc} (abscissa). Points above and below the abscissa give, respectively, the potential across the basolateral cell membrane and across the apical cell membrane (V_{sc} and V_{cm} in Fig. 2), with vertical bars showing the SEM of V_{sc} or V_{cm}. Note that V_{cm} depolarizes but V_{sc} scarcely changes with increasing I_{sc}. The horizontal error bars represent the SEM of I_{sc} values, grouped (from left to right) in the intervals 0 to 0.7, 1.0 to 1.3, 4.6 to 6.6, and 8 to 11 μA/μF

spontaneous variation among bladders in I_{sc} (Fig. 3). Thus, the value decreased towards zero with increasing I_{sc}, from a maximum of -45 mV at 0.2 μA/μF to a minimum of -5 mV at 7 μA/μF (*see* p. 26 for interpretation). The resting potential across the basolateral cell membrane of the apical cell layer (V_{sc} in Fig. 2) was 41 ± 0.8 mV ($n=28$) on open circuit and scarcely changed with I_{sc} (Fig. 3).

Voltage Scanning

This technique establishes a transepithelial voltage by current passage and then seeks to detect inhomogeneities in the potential field in a plane parallel to the plane of the epithelium, as indicators of low-resistance current pathways. A detailed explanation is given by Frömter (1972, e.g. his Fig. 3). When we scanned either the whole bladder surface or just the edge, we could detect no potential inhomogeneities. However, when a hole

was deliberately poked in the epithelium, a voltage deflection of the expected polarity was seen as the scanning electrode passed over the hole. The absence of potential inhomogeneities under normal conditions permits two conclusions: the junctions do not function as low-resistance current pathways in rabbit urinary bladder; and such edge damage as is present is associated with resistances not significantly smaller than the native membrane resistance. By similar voltage scanning techniques, Reuss and Finn (1974) and Higgins, Cesaro, Gebler and Frömter (1975) similarly concluded that junctions are tight in toad urinary bladder and *Necturus* urinary bladder, respectively, while Frömter and Diamond (1972) were able to detect current leaks over the "leaky junctions" of rabbit gallbladder.

Relationship between Voltage-divider Ratio and I_{sc}

The so-called voltage-divider ratio R_a/R_b was measured as the ratio of cell membrane voltage changes (IR drops) V_a to V_b recorded between an intracellular microelectrode and the mucosal or serosal solution (Fig. 2) when a transepithelial square current pulse of 1-sec duration and 4–5 μA amplitude was passed. Unless R_a or R_b change, the ratio V_a/V_b is expected to be independent of the junctional resistance R_j, according to the model of Fig. 2. The current duration of 1 sec greatly exceeds the membrane time constant. The transepithelial IR step resulting from the 4–5 μA current pulse, ±16 mV, is well within the range in which transepithelial resistance is independent of applied current (Fig. 2 of Lewis & Diamond, 1976). Fig. 4 shows that the resulting voltage-divider ratio is in fact independent of applied transepithelial currents up to transepithelial voltage changes of at least ±55 mV, although such large currents do cause a decrease in transepithelial resistance. This suggests that the decrease in transepithelial resistance at high currents may involve a decrease in junctional resistance rather than in cellular resistance.

The ratio V_a/V_b was found to vary from bladder to bladder over an enormous range, from 0.5 to 30, with a mean value of 10.2 ± 2.9 ($n=49$). This variation was not due to varying damage applied to the apical cell membrane by the microelectrode, but was closely and inversely correlated with variation in I_{sc}. Fig. 5 illustrates this relation by plotting the conductance ratio G_a/G_b (the inverse of the voltage-divider ratio) against I_{sc}. As discussed in the previous paper, the total transepithelial conductance G_T increases with I_{sc} (replotted in Fig. 5), and the form of the relation resembles the increase in G_a/G_b with I_{sc}. Hence the increase in G_t with I_{sc} must be due mostly or wholly to an increase in G_a with I_{sc}: i.e., the transport-

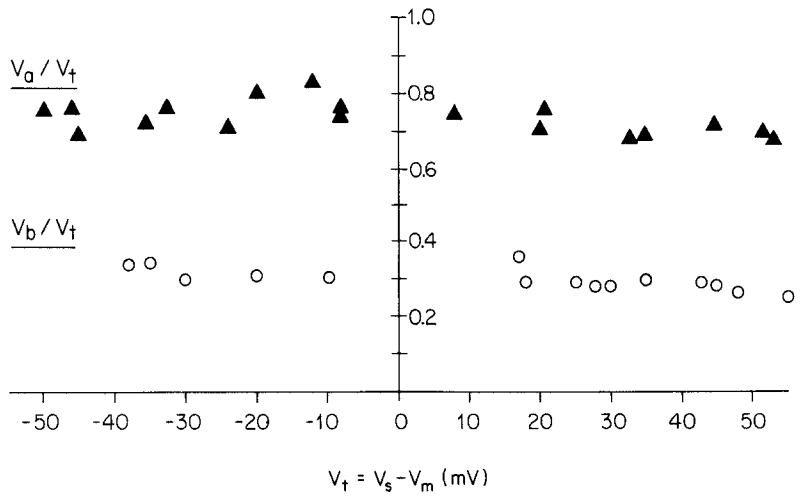

Fig. 4. Voltage-divider ratio α as a function of magnitude and direction of applied transepithelial voltage. V_a/V_t and V_b/V_t are, respectively, the fraction of the transepithelial IR drop recorded between an intracellular microelectrode and the mucosal or serosal bathing solution. Thus, V_a/V_b is α, and $(V_a/V_t)+(V_b/V_t)\sim 1$. Note that neither (V_a/V_t) nor (V_b/V_t) changes significantly with current

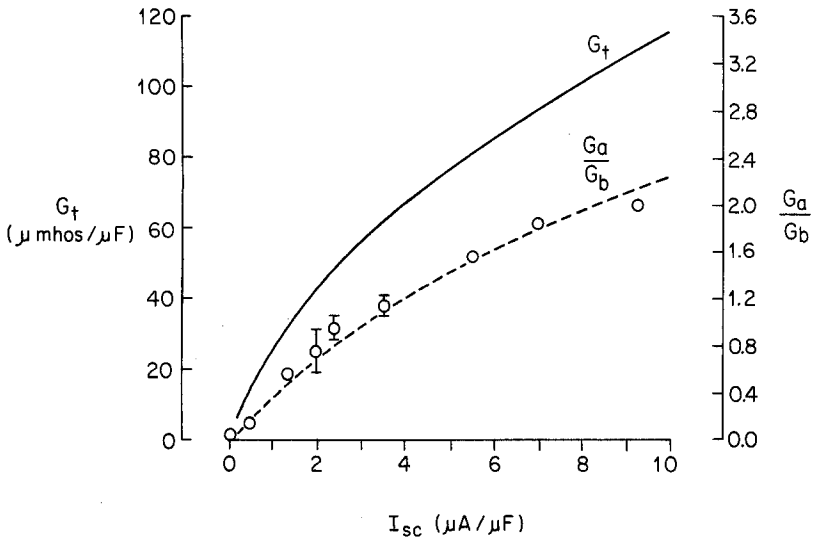

Fig. 5. Transepithelial conductance $G_t(=1/R_t$; solid line above, replotted from Fig. 16 of Lewis & Diamond, 1976) and inverse voltage-divider ratio $G_a/G_b(=1/\alpha$; experimental points and dashed line), as a function of I_{sc}. Experimental points represent values pooled for every 0.5 μA/μF change in I_{sc}, with vertical bars giving SEM only if $n\geqq 3$. Since G_a/G_b as well as G_t increase with I_{sc}, the increase in G_t must be due to an increase in G_a

dependent conductance pathway is in the apical membrane of the apical cell layer. (The possibility of a small contribution from an increase in G_b is not excluded by Fig. 5.)

Does Rabbit Urinary Bladder Exhibit Transverse Cellular Coupling?

Loewenstein, Socolar, Higashino, Kanno and Davidson (1965) demonstrated the existence of low-resistance electrical connections *among* cells of an epithelium, such that current injected into one cell spreads to an adjacent cell. That is, independent of whether cell junctions are tight or leaky in the transepithelial direction, certain junctional structures may serve as cell-to-cell leaks. The structures responsible for cell-to-cell coupling may differ from those responsible for transepithelial tightness or leakiness. If an epithelium consists of a single cell layer, any such current spread or cell coupling can only be within the plane of the epithelium. However, a multi-layered epithelium could have either radial coupling within one cell layer, or transverse coupling between different layers, or both, or neither. For example, Smith (1971) obtained indirect evidence from impedance measurements that there is transverse coupling among the five to seven cell layers of frog skin. The possible existence of transverse coupling among the three cell layers of rabbit urinary bladder is of practical importance in attempts to estimate R_a, R_b and R_j from measurements of radial current spread, for the following reason. If the distance between the voltage-sensing microelectrode and the current-passing microelectrode is less than the effective cell thickness, a correction must be made for nonuniform current density (Eisenberg & Johnson, 1970, pp. 41–44). This effective thickness would be the thickness of one cell layer, ~ 20 μ, if there were no transverse coupling, but could approach the epithelial thickness, ~ 60 μ, if there were transverse coupling. Evidence of transverse coupling was sought by two types of experiments.

Resistance profiles. One approach to detecting transverse coupling would depend on using two microelectrodes simultaneously to impale two cells in different layers, and measuring current spread between layers when current was injected into one layer. As an alternative approach involving only one microelectrode, we advanced an electrode in steps through the epithelium from the mucosal solution while applying transepithelial current pulses (1/sec), and measured the fraction of the transepithelial voltage pulse (the IR drop superimposed on cell resting potentials) recorded by the electrode at each position. This fraction equals the fraction of the transepithelial resistance traversed up to each position.

Fig. 6 depicts four different extremes of theoretical predictions for the dependence of fractional resistance on position, depending on whether transverse coupling is absent (cases 1 and 4) or strong (cases 2 and 3), and on whether the transepithelial resistance of middle and basal layers is significant (cases 1 and 2) or negligible (cases 3 and 4). Four recognizably different forms of the resistance profile are seen to be predicted.

On 15% of the impalements it proved possible to execute this experiment and to measure voltages successively in all three cell layers without damaging the epithelium, as shown by the fact that slow withdrawal of the microelectrode after penetration of the last (most basal) cell layer yielded the same resistance profile as well as sequence of cell resting potentials on the return trip as on the advancing trip. The experiment was performed in the absence of HCO_3^-, so that the transepithelial voltage was virtually zero. In transversing the epithelium, the electrode always first entered a negative potential well [-40 ± 1.6 mV ($n=20$) with respect to the mucosal solution]. On further advance of the electrode, the potential went to zero. With continued advance, in 60% of impalements the electrode entered a second negative well [-42 ± 1.5 mV ($n=12$)], followed by zero, and then in 35% of impalements a third negative well [-42 ± 1.5 mV ($n=7$)], and finally zero again. In three of the seven impalements where three negative wells were seen as the electrode advanced (i.e., in 15% of all impalements) the same three wells were seen as the electrode was withdrawn, while in the other four such impalements cells were torn out as the electrode was withdrawn. We interpret the three wells as the resting potentials of the three successive cell layers, and the two intervening zero-potential regions as the spaces between the first and second or second and third cell layers, respectively. Since one would expect it to be difficult to penetrate all three cell layers without causing damage, we consider the observation of the three steps in "only" 35% of impalements, and of the same three steps during withdrawal of the electrode in "only" 15% of impalements, miraculous rather than disturbing.

Fig. 6 depicts the experimental resistance profile, identifying the electrode position by the resting potential profile as interpreted in the preceding paragraph. The experimental profile fits the theoretical case 4, suggesting two conclusions. First, transepithelial resistance is virtually entirely concentrated in the first cell layer and is negligible for the middle and basal layers, though we cannot discriminate whether this is because these layers have very leaky junctions or else very leaky cell membranes. Second, there is no detectable transverse coupling, although a coupling resistance of less than about 100,000 $\Omega\,\mu F$ might have been detectable.

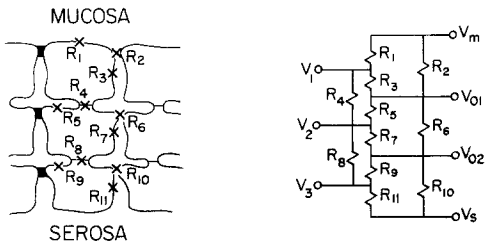

RESISTANCE (kΩ uF)

CASE	R_1	R_2	R_3	R_4	R_5	R_6	R_7	R_8	R_9	R_{10}	R_{11}
1	10	200	6.5	∞	10	200	6.5	∞	10	200	6.5
2	10	200	6.5	10	10	200	6.5	10	10	200	6.5
3	10	200	6.5	10	10	0.3	6.5	10	10	0.3	6.5
4	10	200	6.5	∞	10	0.3	6.5	∞	10	0.3	6.5

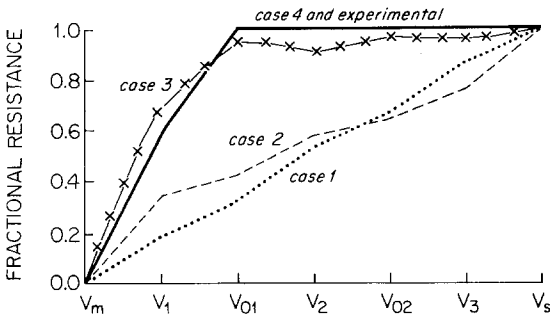

Fig. 6. Theoretical and experimental resistance profiles in rabbit urinary bladder. Above left, sketch of the three-layered epithelium, and above right, corresponding electrical circuit. The 11 resistors are the junctional resistances (in the transepithelial direction) R_2, R_6 and R_{10}, apical membrane resistances R_1, R_5 and R_9, and basolateral membrane resistances R_3, R_7 and R_{11} of the three cell layers; and the transverse coupling resistance R_4 (between the apical and middle layers) and R_8 (between middle and basal layers). Electrode positions are designated as in mucosal (V_m) or serosal (V_s) solutions, intracellularly in each of the three cell layers (V_1, V_2 or V_3), and in the spaces between apical and middle (V_{01}) or between middle and basal (V_{02}) layers. Below, predicted resistance profiles as microelectrode advances from mucosal solution V_m through positions V_1, V_{01}, V_2, V_{02}, V_3 to serosal solution V_s. The profile is expressed as the fraction $(V_x - V_m)/(V_s - V_m)$ traversed up to each point x, where V_x is the IR step at point x in response to a transepithelial current pulse. The four theoretical curves are calculated for the four cases defined by the resistance values displayed in the box in the middle of the Figure: transverse coupling absent (cases 1 and 4) or strong (cases 2 and 3), transepithelial resistances of middle and basal layers high (cases 1 and 2) or negligible [cases 3 and 4; transepithelial resistance of these layers is varied by varying their junctional resistances, but variation in their cell membrane resistances would yield similar profiles (in case 4, though not in case 3)]. The experimental resistance profile below (heavy solid line) coincides with the theoretical curve of case 4, which assumes no transverse coupling and virtually all transepithelial resistance concentrated in the apical cell layer

Thus, although rabbit urinary bladder has three cell layers, it is functionally equivalent to a single-layer epithelium. In all the remaining experiments to be discussed that involved intracellular recording, the electrode was positioned in the first potential well reached from the mucosal solution, hence presumably in the first (apical cell layer). We do not know the function of the middle and basal layers. They are not germinal layers, since the apical layer replaces loss of its own cells by fission of adjacent cells (Walker, 1959). Conceivably, the middle and basal layers may serve in addition to connective tissue to support the apical layer; or else they might deform readily during distension or micturition and thereby reduce strain on junctional complexes and desmosomes. In the remainder of this paper the middle and basal layers will not be discussed further, and the expressions "apical membrane" and "basolateral" membrane will be understood to refer to these cell membranes of the apical cell layer.

Relation between capacitance and I_{sc}. Measurement of the $C_t - I_{sc}$ relation offers a second test of the existence of transverse coupling, for the following reason. The time constant τ for transepithelial voltage response to a square transepithelial current pulse depends on the cell membrane resistances R_a and R_b and capacitances C_a and C_b [Lewis & Diamond, 1976, Eq. (1)]. If an effective transepithelial capacitance C_t is calculated from measurements of τ and transepithelial resistance R_t, as $C_t = \tau/R_t$, a change in R_a or R_b may change the calculated value of C_t, depending on the value of the ratio C_b/C_a. But R_b/R_a does vary widely depending on the value of I_{sc} (Fig. 5). Fig. 7*a* shows that the value of C_b/C_a affects markedly the predicted form of the relation between C_t and I_{sc}, calculated from the known relation between R_b/R_a and I_{sc} and from the assumption that R_b is approximately independent of I_{sc} (p. 19). The actual value of C_b/C_a in rabbit bladder will depend on whether there is transverse coupling. If there is no transverse coupling and if the various cell membranes share capacitance values of about 1 $\mu F/cm^2$ (Fettiplace, Haydon & Andrews, 1971), then C_b/C_a for an electrode in the most apical cell layer should simply be the ratio of the area of that layer's basolateral membrane to its apical membrane. Micrographs (e.g., Fig. 1 of Lewis & Diamond, 1976) suggest that this area ratio is about 2–4. However, if transverse coupling exists, the effective value of C_b could include the capacitances of both membranes of the middle and basal cell layers as well as of the basolateral membrane of the apical layer. Thus, C_b/C_a could be up to 15.

The test was performed by measuring R_t and τ, hence calculating C_t, in eight bladders before and after inhibition of I_{sc} with amiloride. The forms of the voltage time course after a square current pulse did not differ

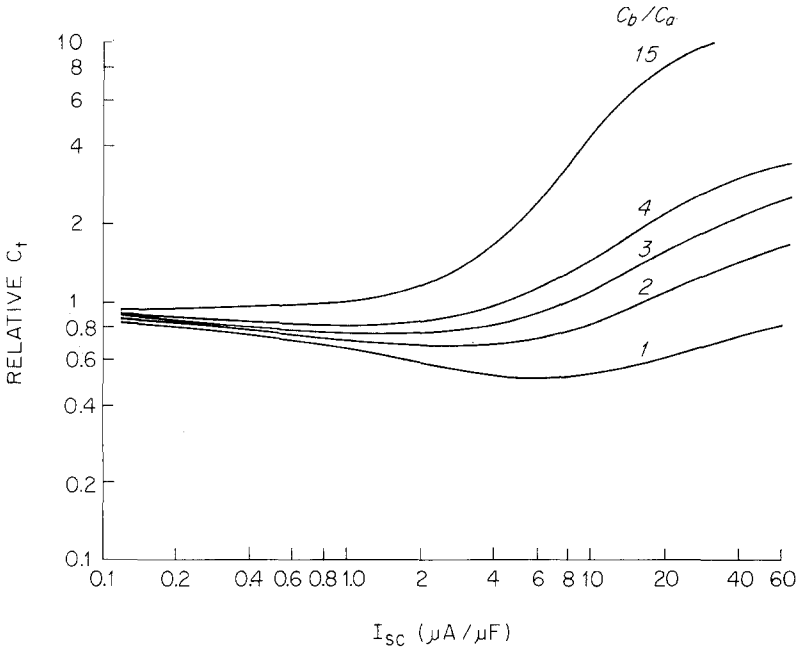

a

Fig. 7*a*. Predicted dependence of effective transepithelial capacitance C_t (ordinate), as a function of I_{sc} (abscissa) and ratio of basolateral to apical membrane capacitances C_b/C_a (written beside each curve). R_b was assumed constant at 7000 Ω cm^2 (*cf.* Tables 2–5), and R_a was calculated from the abscissa value of I_{sc} using this R_b value and the experimental R_b/R_a-*vs.*-I_{sc} relation of Fig. 5. The effective transepithelial time constant τ was then calculated (*see* Appendix of Lewis & Diamond, 1976) as the time to achieve a fraction $(1-1/e)$ of the steady-state transepithelial voltage following a square current pulse across a series combination of apical and basolateral membranes with these R_a and R_b values and the assumed C_b/C_a ratio. Finally, C_t at the given I_{sc} was calculated as $\tau/(R_a+R_b)$, and is expressed on the abscissa as the fraction of the C_t value calculated at $I_{sc}=0$. Note that C_t is expected to change with I_{sc}, and that the form of the relation depends on the value of C_b/C_a. (*b*) Measured effective transepithelial capacitance C_t of frog skin (ordinate), as a function of I_{sc} (abscissa), based on unpublished observations of Lewis and Clausen. Decreases in I_{sc} below the spontaneous value were produced by adding amiloride to the mucosal bathing solution. Note that C_t obviously increases with I_{sc}, as predicted theoretically in part *a* for large values of C_b/C_a. The scales are logarithmic in part *a*, linear in part *b*. Frog skin does in fact have a large C_b/C_a value because of transverse coupling (Smith, 1971), taking into account that R_b for frog skin is less than half the value assumed in part *a*

markedly from single exponentials. As summarized in Table 1, amiloride caused a small decrease in C_t in seven of the eight bladders, the exception being the bladder with the lowest spontaneous I_{sc} and proportionately smallest amiloride effect on I_{sc}. For each experiment the pairs of values of I_{sc} and of *relative* C_t, before and after amiloride, were matched to the theoretical curves of Fig. 7*a*, to determine which curve predicted most

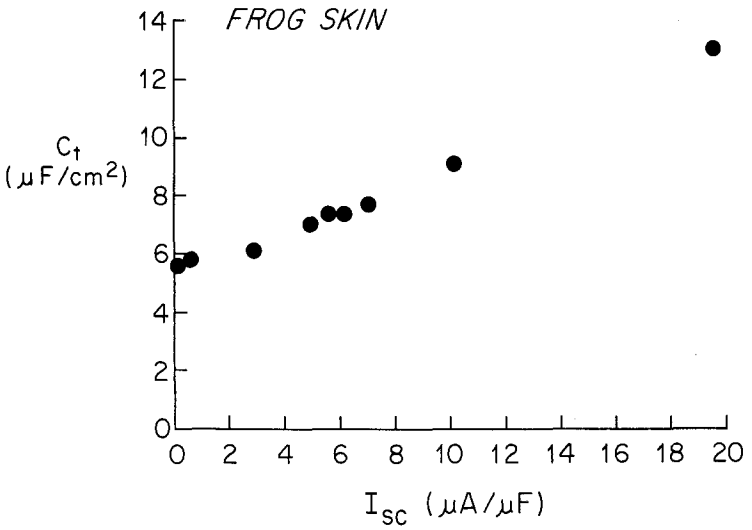

Figure 7b

closely the relative effect of amiloride on C_t. The resulting best-fit values of C_b/C_a (last column of Table 1) were all in the range 2–4, with an average value of 2.6 ± 0.3. This value is in agreement with the assumption of no transverse coupling, and hence with the conclusion drawn from the resistance profile measurement of Fig. 6. Obviously, the observed capacitance changes of Table 1 are not much beyond the error limits of experimental measurement, and this experiment does not by itself provide compelling support for our interpretation. In contrast, the increase in C_t with I_{sc} for frog skin, as illustrated in Fig. 7*b* (Lewis & Clausen, *unpublished observation*), is large and obvious: C_t at the highest I_{sc} value of 19.6 μA/μF is more than double that at the lowest current of 0.1 μA/μF. The reason why the effect is much more marked in frog skin than in rabbit bladder follows from the differences in transverse coupling in these preparations, and from Fig. 7*a*. This theoretical figure shows that the deviation from 1.0 of the ratio of C_t at high current to C_t at low current is slight if $C_b/C_a \sim 3$, but is large if $C_b/C_a \sim 15$ or higher. In rabbit bladder, where there is no transverse coupling, C_b/C_a just equals the ratio of basolateral membrane area to apical membrane area for the apical cell layer, or about 3. In frog skin, transverse coupling does exist among the many cell layers, so that all subapical cell layers contribute to C_b, and the estimated value of C_b/C_a is 50 (Smith, 1971).

Intracellular current-voltage relation. A prerequisite for cable analysis of spread of intracellularly injected current through the epithelium is to

Table 1. Change in effective capacitance with I_{sc}

I_{sc}(μA/μF)		C_t(μF/cm^2)		$\frac{C_t(\text{before})}{C_t(\text{after})}$	C_b/C_a
before amiloride	after amiloride	before amiloride	after amiloride		
2.4	1.18	1.25	1.27	0.98	3
4.3	0.91	1.29	1.37	0.94	2
5.5	0.83	1.76	1.80	0.98	2
1.28	1.01	1.95	1.87	1.04	4
1.66	0.90	1.60	1.62	0.99	3
1.31	0.80	1.19	1.28	0.93	2
3.1	1.08	1.89	1.94	0.97	3
1.42	0.68	1.37	1.47	0.93	2

I_{sc} (columns 1 and 2) and effective transepithelial capacitance (columns 3 and 4) were measured before and after addition of amiloride (10^{-4} M) to inhibit transport and increase R_a. Each row represents an experiment on a different bladder. The last column is the value of C_b/C_a corresponding to that theoretical curve of Fig. 7*a* which best predicts the ratio C_t(before)/C_t(after) for the given pair of I_{sc} values. This best-fit C_b/C_a is 2.6 ± 0.3 (average ± SEM).

establish the current range over which the cellular voltage response is linear. To determine this range, we passed a current ramp between an intracellular microelectrode and the grounded mucosal solution, and recorded the apical-membrane potential V_{cm}. Since the membrane time constant is 10–20 msec but the ramp duration was 10 sec, the voltage response to the ramp would be virtually linear if the cell membrane I-V relation were linear. Fig. 8 shows that the response is very nonlinear: cellular resistance is much higher for depolarizing currents (segments 3 and 4) than for hyperpolarizing currents (segments 1 and 2). The same conclusion followed when we used 1 sec current pulses instead of current ramps. With successive ramps, rectification appears at successively smaller depolarizing currents (compare segments 3 and 4), and the I-V slope (the resistance in the hyperpolarizing direction) also increases (compare segments 5 and 1–2).

Fig. 9 illustrates predictions of two hypotheses to explain this nonlinear cellular I-V relation. The hypotheses must also account for the nonlinear but symmetrical transepithelial I-V relation (Fig. 2 of Lewis & Diamond, 1976), and for the fact that the voltage-divider ratio is independent of direction or magnitude of applied transepithelial current (Fig. 4).

Hypothesis 1. The apical cell membrane resistance R_a behaves as a rectifier, but the basolateral membrane resistance R_b does not. This

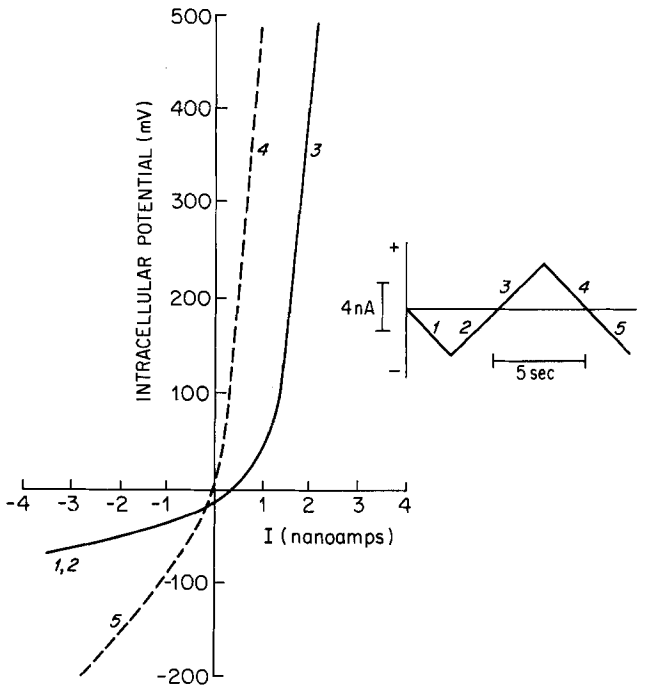

Fig. 8. Intracellular voltage response (left, ordinate) to intracellularly injected current (left, abscissa) applied as a current ramp of the form shown on the right. Ramps 1–4, as designated in the right-hand sketch, were applied several times in immediate succession until successive I–V relations became approximately the same, at which point the series was then terminated with ramps 1 (="5") and 2. The numbers on the intracellular I–V relation (left) indicate which segment corresponds to which part of the current ramp. The I–V relation obtained by the first application of ramps 1–3 (solid line, left) is identical in form to the I–V relation obtained by 1-sec square current pulses of different magnitudes separated by long times. "2" beside the solid line means that segments 1 and 2 of the first ramp give identical I–V relations. Note that the depolarizing slope (segments 3 and 4) is steeper than the hyperpolarizing slope (segments 1–2 and 5), and that successive ramps shift the form of the I–V relation (segments 4 and 5 *vs.* 1–2 and 3), for reasons discussed in the text

hypothesis accounts for the rectifying cellular I-V relation, but it incorrectly predicts a rectifying transepithelial I-V relation and a current-dependent voltage-divider ratio, and it fails to account for the time dependence of rectification during successive ramps. The complementary hypothesis, that R_b rectifies and R_a does not, suffers from the same deficiencies, as does in general the hypothesis that both resistors rectify.

Hypothesis 2. Individual cell membranes do not rectify, but depolarizing current interrupts cell-to-cell coupling, with a certain time constant for interruption and another time constant for restoration of coupling after cessation of the depolarizing current. With coupling intact, injected

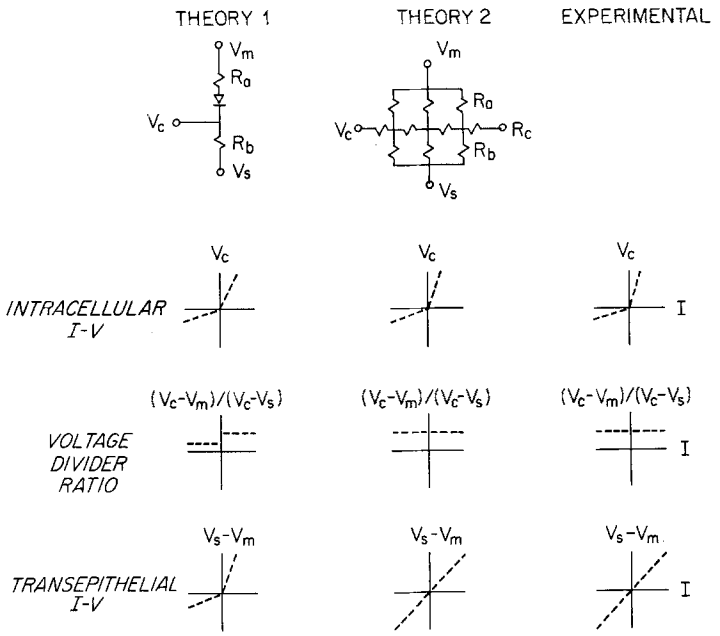

Fig. 9. Comparison of experimental results (right) and two theoretical predictions (left) for forms of the intracellular current-voltage relation (second row; intracellularly injected current passed simultaneously to both bathing solutions), dependence of voltage-divider ratio α on transepithelial current (third row), and transepithelial current-voltage relation (last row). Junctional resistors are assumed infinite in all three theoretical circuits. Theory 1: the apical membrane resistor R_a rectifies, the basolateral membrane resistor R_b does not. The intracellular and transepithelial I–V relations will both be asymmetrical, and α will depend on current direction. Theory 2: neither the apical nor the basolateral membrane rectifies, but cells are coupled through a resistor that does rectify. The intracellular I–V relation will be asymmetrical, α constant, and transepithelial I–V relation symmetrical. The experimental results fit theory 2

current would spread through the epithelium (Fig. 10) and the measured cell resistance would be the reciprocal summed conductance of many cells. With coupling interrupted, the measured resistance would approach that of a single cell. This hypothesis correctly predicts a rectifying and time-dependent cellular I-V relation, current-independent voltage-divider ratio, and symmetrical transepithelial I-V relation.

Further support for this attribution of cellular rectification to uncoupling comes from *Chironomus* salivary gland, where depolarizing currents similarly uncouple cells with a time constant of 0.1–4.0 sec, depending on the current strength (Socolar & Politoff, 1971). The following observation suggests that the uncoupling time constant in rabbit bladder may be in the range 0.2–0.5 sec. Intracellular injection of square depolar-

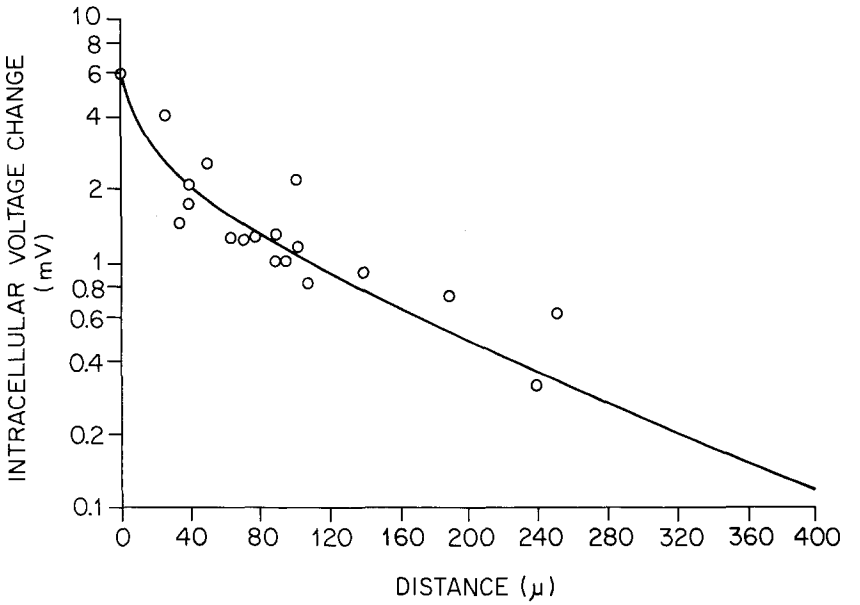

Fig. 10. Radial spread of intracellularly injected current: the intracellular voltage change in response to an injected current pulse (ordinate, logarithmic scale), as a function of distance from the injection cell (abscissa). Each point represents a voltage measurement in a different cell. The line fitted through the experimental points is the best fit of the Bessel function, Eq. (3) of the text

izing current pulses yielded, for small currents, a steady maintained voltage response (after a 10–20 msec capacitative rise-time); at some larger threshold current, appearance of voltage oscillations; and, for larger currents, a rapid drastic increase in voltage after 0.2–0.5 sec, presumably due to the development of uncoupling. Cell uncoupling with depolarizing intracellular currents will be used as the basis of a method for estimating cell membrane resistances without resort to cable analysis (p. 19).

Values of Cell Membrane and Junctional Resistances

Four methods were used to determine R_a, R_b and R_j.

1. *Method 1: Cable Analysis.* Frömter (1972), Frömter and Diamond (1972), Spenney, Shoemaker and Sachs (1974), and Reuss and Finn (1974) have used cable analysis to measure R_a, R_b and R_j in flat epithelial sheets. These parameters may be extracted from three measurements: the transepithelial resistance R_t, voltage-divider ratio $R_a/R_b = \alpha$, and resistance R_z to current flow from an intracellular electrode to the bathing solutions. Because of cell coupling, intracellularly injected current spreads radially

to other cells from the origin cell. In an infinite plane the equation for radial dependence of voltage $V(x)$, following Shiba (1971) and Frömter (1972), is

$$\frac{d^2V}{dx^2}+\frac{1}{x}\frac{dV}{dx}-\frac{V}{\lambda^2}=0 \tag{2}$$

where x is the radial distance within the plane from the current-injection site. The solution to this equation under our boundary conditions is

$$V(x)=AK_0(x/\lambda) \tag{3}$$

where K_0 is a zero-order modified Bessel function of the second kind, the length constant λ equals $\sqrt{R_z/R_x}$, and R_x is the resistance to current flow within the plane in the radial direction (cell coupling resistance plus cytoplasmic resistance). Experimental measurements of $V(x)$ against x were fitted to Eq. (2) by a nonlinear least-squares curve-fitting package (Brown & Dennis, 1972), using APL*PLUS language (registered trademark of Scientific Time Sharing Corporation, Bethesda, Md.) and an IBM 360/91 computer, to obtain the values of A and λ. R_x and R_z were then calculated as

$$R_x=2\pi A/I_0 \tag{4}$$

$$R_z=2\pi A\lambda^2/I_0 \tag{5}$$

where I_0 is the injected current. Since R_z is determined by the resistors R_a and R_b in parallel[1] ($R_z=R_aR_b/(R_a+R_b)$), we finally calculate R_a, R_b and R_j as

$$R_a=(1+\alpha)R_z \tag{6}$$

$$R_b=(1+\alpha)R_z/\alpha \tag{7}$$

$$R_j=(R_tR_a+R_tR_b)/(R_a+R_b-R_t).$$

Fig. 10 illustrates experimental measurements of $V(x)$ against x, and the line fitted by Eq. (2). Radial current spread proved small but symmetrical and did not exhibit preferential directions of coupling as reported by Loewenstein *et al.* (1965) for toad bladder. We were able to complete only two successful cable analyses, because the bladder had to be stretched somewhat to approximate a flat sheet so that optical measurements of x would be meaningful. In other attempts this stretch uncoupled the bladder cells, an effect that was not reversed by placing mineral oil on the mucosal

1 Although injected current is passed between the cell and the mucosal solution, the mucosal and serosal solution behave for the purposes of this experiment as if shunted, since R_t of the whole epithelium is several hundred times smaller than the effective R_b of the patch of epithelium through which injected current spreads. Thus, R_z does not equal R_a alone but is determined by R_a and R_b in parallel. See Frömter (1972, pp. 264, 284 and 295-6) for further explanation.

Table 2. Bladder electrical parameters from method 1 (cable analysis)

I_{sc} ($\mu A/\mu F$)	α	A (mV)	λ (μ)	I_0 (μA)	R_x (Ω)	R_z ($\Omega\,\mu F$)	R_t ($\Omega\,\mu F$)	R_a ($\Omega\,\mu F$)	R_b ($\Omega\,\mu F$)	R_j ($\Omega\,\mu F$)
1.3	2.03	10.9	165	0.0038	1.80×10^7	4,900	11,000	14,900	7,300	21,600
1.1	2.33	1.12	185	0.00045	1.56×10^7	6,900	8,000	23,200	9,000	10,500

Each row represents a different bladder, with the I_{sc}, α and R_t values given in columns 1, 2 and 8. A and λ were calculated from the best fit of the Bessel function Eq. (3) to the radial dependence of voltage during intracellular injection of current I_0 (column 5). R_x and R_z were calculated from A, λ and I_0 by Eqs. (4) and (5). R_a, R_b and R_j were calculated from α, R_z and R_t by Eqs. (6), (7) and (8). R_j values are relatively low, due to edge damage caused by the microelectrode chamber.

surface, as reported by Reuss and Finn (1974) for toad bladder. Table 2 summarizes the results. In these particular bladders, which happened to have relatively low values of I_{sc}, R_a exceeds R_b.

2. *Method 2: Resistance of Uncoupled Cells.* We had to resort to cable analysis to extract membrane resistances of bladder because the bladder's cells are normally coupled, provided that intracellularly injected current is in the hyperpolarizing direction. However, the nonlinear I–V relation of Fig. 8 and the accompanying discussion indicate that depolarizing currents uncouple cells. With successive current ramps the current-voltage relation becomes increasingly steep, approaches linearity, and eventually keeps the same form with further ramps. We interpret this to mean that cells are now completely uncoupled, and that the resistance calculated as the slope $\Delta V/\Delta I_0$ of the current-voltage relation in this condition now applies to a single cell. Multiplying this slope by $2\pi r^2$, where the cell membrane is approximated as two parallel flat discs (apical membrane and basolateral membrane) of radius 15 μ (from light micrographs), yields the cell membrane resistance R_z in units $\Omega\,cm^2$ as $2\pi r^2 \Delta V/\Delta I_0$. Finally, measurement of α and R_t, and application of Eqs. (6–8), yields the values of R_a, R_b and R_j calculated for seven bladders in Table 3. The obvious conclusion of Table 3 is that R_a varies inversely with I_{sc}, supporting the conclusion drawn from Fig. 6 and from the rapid effect of amiloride added to the mucosal solution that the transport-dependent conductance pathway is located in the apical membrane.

Method 3: Pairs of Values of R_t and α. If the preceding sentence is correct, then the variation in R_t with I_{sc} demonstrated by many different experimental manipulations (Fig. 5; also, Lewis & Diamond, 1976, Fig. 16) might be due entirely to variation in R_a and not at all to variation in R_b

Table 3. Bladder electrical parameters from method 2 (uncoupled cells)

I_{sc} (μA/μF)	α	ΔV (mV)	I_0 (μA)	R_{cell} (Ω)	R_z (Ω μF)	R_t (Ω μF)	R_a (Ω μF)	R_b (Ω μ F)	R_j (Ω μF)
3.5	2.27	35	0.0001	3.5×10^8	4,900	10,300	16,200	7,100	10,500
2.75	4.2	21	0.00007	3.0×10^8	4,200	5,500	22,000	5,300	7,000
2.75	4.2	63.5	0.00015	4.2×10^8	6,000	5,500	29,000	6,900	6,500
–	5.2	28	0.00007	4.0×10^8	5,700	5,800	36,700	6,700	6,600
2.25	11	15	0.00004	3.75×10^8	5,300	7,900	63,600	5,800	8,900
0.55	12	157	0.00025	6.3×10^8	8,900	10,800	115,000	9,600	12,000
0.50	17.5	27.5	0.00005	5.5×10^8	7,800	11,000	144,000	8,200	12,000

Successive current ramps were injected intracellularly until the I-V relation became linear and reached an asymptotic slope, suggesting interruption of cell-to-cell coupling. Each row represents a different bladder, with the I_{sc}, α and R_t values given in columns 1, 2 and 7. The resistance of a single cell, R_{cell} (column 5), was calculated as the ratio of its voltage response ΔV (column 3) to the injected depolarizing current I_0 (column 4). R_z was calculated as $2\pi r^2 R_{cell}$, approximating a cell as two flat discs and taking r as 15 μ. R_a, R_b and R_j were calculated from α, R_z and R_t by Eqs. (6), (7) and (8). R_j values are relatively low, due to edge damage caused by the microelectrode chamber. Note that R_a increases nearly 10-fold with decreasing I_{sc}.

or R_j. Two pairs of measured values of R_t and α in the same bladder, corresponding to two different I_{sc} values (e.g., before and after amiloride) and designated by superscripts $'$ and $''$, could then be formulated as

$$\begin{aligned} R_t' &= R_j R_b(\alpha'+1)/[R_j + R_b(\alpha'+1)] \\ R_t'' &= R_j R_b(\alpha''+1)/[R_j + R_b(\alpha''+1)]. \end{aligned} \tag{9}$$

These two simultaneous equations may be solved for R_j and R_b, then R_a corresponding to each pair of values (R_t, α) is calculated as αR_b. In support of the assumption that amiloride affects only the transport-dependent conductance pathway, we found that amiloride had no effect on R_t in choline solutions, where I_{sc} is zero. This method was developed independently by Reuss and Finn (1974).

Table 4 summarizes values of R_a, R_b and R_j calculated in this way for five bladders in which R_t and α were measured before and after amiloride.

Method 4: R_t vs. I_{sc}, and α vs. I_{sc}. The previous three methods all involve simultaneous measurement of R_t and α in our microelectrode chamber. Compared to the chamber design used in the preceding paper for transepithelial measurements, our microelectrode chamber design caused some edge damage, as shown by two facts: R_t values with this chamber are lower (5,000–25,000 Ω μF compared to the values of 7,000–78,000 Ω μF obtained in the preceding paper); and the values of R_j obtained by methods

Table 4. Bladder electrical parameters from method 3 (pairs of α, R_t values)

Experiment	I_{sc} ($\mu A/\mu F$)	α	R_t ($\Omega\,\mu F$)	R_a ($\Omega\,\mu F$)	R_b ($\Omega\,\mu F$)	R_j ($\Omega\,\mu F$)
1	3.5	0.60	7,400	3,700	6,200	31,000
	1.7	1.07	9,000	6,600		
2	0.7	9	18,000	44,600	5,000	28,300
	0.0	31	24,000	154,000		
3	1.7	1.07	12,000	10,600	9,900	30,700
	0.5	5	20,000	49,500		
4	3.7	1.00	10,200	7,200	7,200	34,500
	0.5	5	19,200	36,200		
5	3.7	0.67	7,400	4,100	6,100	27,800
	2.4	1.20	9,000	7,300		

Each of five bladders is represented by two rows of entries: the upper and lower rows give, respectively, before and after amiloride, the values of I_{sc}, α and R_t. R_a, R_b and R_j (last three columns) were calculated from the two pairs of α and R_t values by Eq. (9) which assumes that the increase of α and R_t with decreasing I_{sc} is due to an increase of R_a. R_j is relatively low, due to edge damage caused by the microelectrode chamber.

1–3, 6,500–35,500 $\Omega\,\mu F$, are lower than maximal total transepithelial resistances R_t obtained in the preceding paper after amiloride, 78,000 $\Omega\,\mu F$. Edge damage is expected not to affect measured α's or I_{sc}'s but to reduce measured R_t's and R_j's, since edge-damage conductance cannot be distinguished from junctional conductance by the first three methods. (Nevertheless, this edge-damage conductance was still too small to detect in the voltage-scanning experiment.)

Therefore, method 4 depends on the same principles as method 3 but uses R_t values measured in the preceding paper without the microelectrode chamber. This was achieved as follows. Fig. 5 gives the experimental relation between α and I_{sc}, both measured in the microelectrode chamber (but both quantities are expected not to be affected by edge damage). Fig. 16 of the previous paper (reproduced as the upper curve of Fig. 5 of this paper) gives the experimental relation between G_t and I_{sc}, both measured without the microelectrode chamber. The $G_t - I_{sc}$ relation was then used to transform the I_{sc} axis of the $\alpha - I_{sc}$ relation into a G_t axis, yielding the $\alpha - G_t$ relation. Furthermore, Eq. (1), reexpressed in terms of conductances instead of resistances becomes

$$G_t = G_j + G_a G_b/(G_a + G_b) \quad \text{or} \quad G_t = G_j + G_b/(1+\alpha). \tag{10}$$

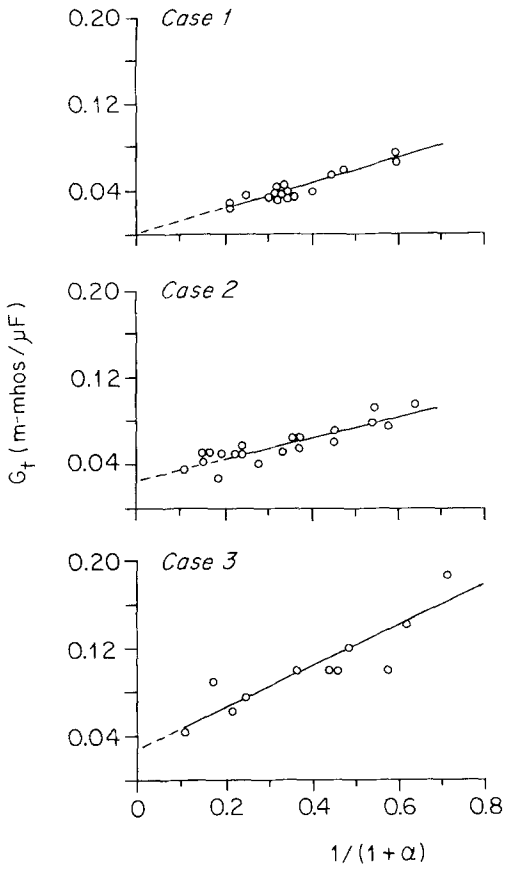

Fig. 11. Transepithelial conductance G_t (ordinate), plotted against $1/(1+\alpha)$ (abscissa), where α was read off from the lower curve of Fig. 5 at the transport rate I_{sc} corresponding to this G_t value (upper curve of Fig. 5). As discussed in the text, the slope of each curve is G_b, and the ordinate intercept is G_j (junctional plus edge-damage conductance). Case 1: silicone sealant, membrane not highly stretched. Case 2: vaseline sealant, membrane not highly stretched ($C_t > 1.1$ μF/cm^2). Case 3: vaseline sealant, highly stretched membrane ($C_t < 1.1$ μF/cm^2 chamber area). Note that the slopes are the same in cases 1 and 2 and higher in case 3; and that the ordinate intercepts are the same in cases 2 and 3 but almost zero in case 1, indicating elimination of edge damage by silicone sealant

Eq. (10) states that, if G_a but not G_b or G_j varies with I_{sc}, a graph of G_t versus $1/(1+\alpha)$ should yield a slope of G_b and intercept of G_j.

By starting with the $\alpha - G_t$ relation and transforming the α axis into a $(1+\alpha)^{-1}$ axis, Fig. 11 depicts the experimental results in the form of Eq. (10). The results are shown for three different mounting techniques: case 1, our usual method using silicone sealant; case 2, vaseline sealant, and the bladder not highly stretched (i.e., $C_t > 1.1$ μF/cm^2 chamber area); case 3,

vaseline sealant, the bladder highly stretched (i.e., $C_t < 1.1$ μF/cm2). All three graphs approximate straight lines, supporting the assumption that transport-related conductance changes are mainly in G_a. However, there are differences among the three cases in the slopes G_b and intercepts G_j.

In the cases 2 and 3, which differ only by stretch, $R_j (= G_j^{-1})$ is virtually the same (38,000 and 36,000 kΩ μF, respectively). Evidently, stretch does not affect R_j but decreases R_b. $R_b (= G_b^{-1})$ is significantly lower in the stretched preparation (5,300 *vs.* 10,300 kΩ μF). However, we cannot be certain that this apparent decrease of R_b with stretch is real, because values of α were not measured in the more highly stretched preparations but were assumed equal to those of the less stretched preparations. The value of α affects the estimate of R_b but not of R_j.

In cases 1 and 2, which differ only by sealant, R_b is essentially the same (8,600 *vs.* 10,300 Ω μF). The intercept in case 1 is much lower than in cases 2 or 3 and does not differ significantly from zero, corresponding to $R_j \sim 300{,}000$ Ω μF or not significantly different from infinite. Evidently, silicone virtually eliminates edge damage whereas vaseline does not—as also concluded in the preceding paper from the fact that silicone yields consistently higher values of R_t.

Discussion

We begin this section by comparing our values for R_b, R_j and R_a as obtained by the four different methods (Table 5). The results of this and the preceding paper are then assembled into a possible model of Na transport that may also apply to some other "tight" epithelia (Lewis, Clauson & Diamond, 1975).

Values of R_b, R_j and R_a

R_b. The values obtained from the four methods are in good agreement, given the major differences among the methods and errors (Table 5). Assuming that 1 μF corresponds to *ca.* 1 cm^2 apical membrane area, then R_b is *ca.* 5,000–10,300 Ω cm^2. For comparison, R_b is 2,900 Ω cm^2 for *Necturus* gallbladder, a leaky epithelium (Frömter & Diamond, 1972); 4,000 Ω cm^2 for *Necturus* stomach, a tight epithelium (Spenney *et al.*, 1974); 2800–3600 Ω cm^2 for toad urinary bladder, another tight epithelium (Reuss & Finn, 1974); and 5000 and 2500 Ω μF for frog skin and bladder, respectively (Lewis *et al.*, 1975). The specific resistance related to actual area of basolateral membrane is considerably higher, since the ratio of basolateral to apical membrane area exceeds 1. Taking this ratio as 2.6 for

Table 5. Comparison of bladder electrical parameters estimated by four different methods

Method	I_{sc} (μA/μF)	R_a (Ω μF)	R_b (Ω μF)	R_j (Ω μF)
1	1.3	14,900	7,300	21,800
1	1.1	23,200	9,900	10,500
2	3.5	16,200	7,100	10,500
2	2,75	22,000	5,300	7,000
2	2.75	29,000	6,900	6,500
2	—	36,700	6,700	6,600
2	2,25	63,600	5,800	8,900
2	0.55	115,000	9,600	12,000
2	0.50	144,000	8,200	12,000
3	3.7	4,100	6,100	27,800
3	3.7	7,200	7,200	34,500
3	3.5	3,700	6,200	31,000
3	2.4	7,300	6,100	27,800
3	1.7	6,600	6,200	31,000
3	1.7	10,600	9,900	30,700
3	0.7	44,600	5,000	28,300
3	0.5	36,200	7,200	34,500
3	0.5	49,500	9,900	30,700
3	0.0	154,000	5,000	28,300
4 (silicone sealant)	5.2	5,150	8,600	∞
	0.7	36,400	8,600	∞
4 (vaseline, not stretched)	6.9	3,850	10,300	38,500
	0.3	80,000	10,300	38,500
4 (vaseline, stretched)	11.7	2,300	5,400	35,700
	0.25	91,000	5,400	35,700

The values are assembled from Tables 2, 3 and 4 and Fig. 11. Note that, by each method, R_a increases with decreasing I_{sc}, while R_b and R_j show little correlation with I_{sc}.

rabbit urinary bladder, we obtain $R_b \sim 13{,}000$–$27{,}000\ \Omega\ cm^2$ for rabbit urinary bladder. Thus, by comparison with the orders-of-magnitude differences among epithelia in their R_a or R_j values, as discussed in the following paragraphs, R_b values do not differ greatly among the epithelia studied to date. It should be added that our R_b estimate in rabbit urinary bladder included the resistance of everything in series between the interior of the apical cell layer and the serosal solution – i.e., the middle and basal cell layers as well as the basolateral membrane of the apical layer. However, the transepithelial resistance of these lower two cell layers is negligible (Fig. 6), so that in practice our R_b estimate applies to the basolateral membrane of the apical layer.

R_j. With silicone sealant and the chamber used in the preceding paper, R_j is *ca.* 300,000 Ω μF or immeasureably high (Table 5, method 4, case 1).

With vaseline sealant or the microelectrode chamber (Table 4, method 4, cases 2 and 3, or methods 1–3, respectively), R_j varies between 6,500 and 38,000 $\Omega\,\mu F$ and is not correlated with I_{sc}. Thus, essentially all the paracellular conductance measured by these latter methods arises from edge damage or imperfect sealing: these low measured values of "R_j" really do not refer to junctional resistance. In the native bladder essentially all transepithelial conductance is transcellular. In contrast, the junctional resistance in *Necturus* gallbladder, a leaky epithelium, is at least three orders of magnitude lower than in rabbit urinary bladder (324 $\Omega\,cm^2$: Frömter, 1972; Frömter & Diamond, 1972), and 96% of native transepithelial conductance is paracellular. Rabbit urinary bladder appears to represent an upper extreme in R_j even among tight epithelia, but the values reported for other tight epithelia (toad urinary bladder, ~13,000 $\Omega\,cm^2$: Reuss & Finn, 1974; *Necturus* stomach, 20,000 $\Omega\,cm^2$: Spenney *et al.*, 1974) may be underestimates due to edge damage.

Although stretch interrupts cell-to-cell coupling (p. 18), it does not affect R_j (Table 4, Method 4: compare cases 2 and 3). This may support the suggestion that the junctional structures that provide cell-to-cell conductance and those that block transepithelial conductance are different. The lack of effect of stretch on the transepithelial junctional resistance may be physiologically significant, in maintaining high resistance to dissipation of transbladder ion gradients even when the bladder is distended with urine.

R_a. No single value can be given for R_a, since it varies over nearly two orders of magnitude from 3,700 to 154,000 $\Omega\,\mu F$. This variation is inversely correlated with variation in I_{sc}, and accounts for all or nearly all of the observed variation in R_t with I_{sc}. Further evidence for the location of this transport-related conductance pathway in the apical membrane is that concentration changes of amiloride, Ca^{++}, or Na^+ in the mucosal solution affect R_t with a half-time of a few seconds or less. We have observed similar conductance changes in frog skin and frog bladder (Lewis *et al.*, 1975), as have Higgins *et al.* (1975) in *Necturus* bladder.

The Transport Mechanism of Rabbit Urinary Bladder

In order to combine our findings into a model of the transport mechanism, we consider in turn: (1) properties of the apical membrane, (2) properties of the basolateral membrane, (3) feedback from cell (Na^+) to apical membrane conductance, (4) the aldosterone effect, and (5) location of the rate-limiting step. We reiterate that this entire discussion applies

to the apical cell layer, since we found the transepithelial resistance of the other two cell layers to be negligible.

1. *Apical membrane.* At moderate or high transport rates the amiloride-sensitive channel for Na^+ entry accounts for most of the conductance of this membrane, since G_a increases by nearly two orders of magnitude with increasing I_{sc}. However, this membrane must also contain a small leak to K^+, H^+ or Cl^-, since the resting potential at very low transport rates is about -40 mV (cell interior negative). If, by analogy with intracellular ion concentrations estimated for toad urinary bladder (Handler, Preston & Orloff, 1972), (Na^+) and (Cl^-) are lower and (K^+) higher in rabbit bladder cells than in a plasma-like Ringer's solution, then the Na^+ gradient is in the wrong direction, but the K^+, Cl^- and conceivably also H^+ gradients are in the right direction, to account for this resting potential. The decline in resting potential to -5 mV at high transport rates is in the right direction to be attributed to increased G_{Na} associated with the amiloride-sensitive channel. In toad bladder (Reuss & Finn, 1974) and *Necturus* bladder (Higgins & Frömter, 1974) the potential changes with transport rate are in the same direction as in rabbit bladder. However, the potential actually reverses (cell interior positive) at high rates in these other two tissues. We have no reason to suspect that Na^+ entry at the apical membrane is other than down its electrochemical gradient, but in the absence of knowledge of intracellular (Na^+) we cannot prove downhill entry.

2. *Basolateral membrane.* The orientation of the resting potential across this membrane is cell interior negative to serosal solution, at all transport rates observed. Assuming cell (Na^+) to be below that in the serosal solution, Na^+ extrusion across the basolateral membrane must be active and presumably involves the Na^+-K^+-activated, ouabain-inhibited ATPase detected in bladder membrane fragments (Lewis & Diamond, 1976). The 40 mV resting potential at zero transport rate may be a diffusion potential due to the K^+, Cl^- or H^+ gradients; it is assumed to be a K^+ diffusion potential in the Koefoed-Johnsen and Ussing (1958) model.

3. *Negative feedback from cell (Na^+) to apical membrane conductance.* Amiloride and Ca^{++}, which act from the mucosal solution to block Na^+ entry, increase R_t (by increasing R_a) while blocking I_{sc}. But removal of HCO_3^- from the serosal solution also blocks I_{sc} while increasing R_t. Addition of ouabain or the metabolic inhibitors cyanide or Na to the serosal solution also block I_{sc} and (initially) increase R_t, although these agents presumably act on the pump in the basolateral membrane. Hviid Larsen (1973) found similar effects on addition of cyanide and ouabain

to the serosal solution of frog skin, and localized the resistance changes to the apical membrane. Inhibition of Na^+ extrusion at the basolateral membrane increases cell (Na^+), as illustrated by intracellular ion analyses of toad bladder cells before and after ouabain (Handler *et al.*, 1972). Since the simplest effect of increased cell (Na^+) would be to increase G_{Na} in the apical channel for Na^+ entry, the decrease in G_t actually observed suggests a negative feedback mechanism whereby cell (Na^+) inhibits the apical entry channel [a mechanism that has been postulated for frog skin (Ussing, Erlij & Lassen, 1974)]. Such a mechanism is also suggested by the fact that stimulation of Na^+ entry by ADH, inhibition of Na^+ extrusion by ouabain, and stimulation of transport by aldosterone (stimulating Na^+ entry?) all cause cell (Na^+) in toad bladder to rise to about the same value, 52–63 mM (Handler *et al.*, 1972), a value close to the concentration that saturates the Na^+-K^+-ATPase (Bonting, 1970). [There is, however, a conflict between the results of Handler *et al.* (1972) and those of Lipton and Edelman (1971). The values obtained by both of these groups of authors for intracellular (Na^+) does not necessarily represent the so-called "Na^+ transport pool", as shown by the work of MacKnight, Civan and Leaf (1975*a*, *b*).]

The physiological significance of the postulated feedback mechanism may be as follows. For any given perturbation in solution concentration and basolateral Na^+ extrusion rate (or apical Na^+ entry rate), a new steady-state involving a change in cell (Na^+) and volume and in Na^+ entry (or extrusion) rate will eventually be established. A perturbation that caused too large an increase in cell volume might result in cell lysis. This is the probable interpretation of the eventual decrease in R_t observed after ouabain, N_2, cyanide or HCO_3^--free serosal solutions (Lewis & Diamond, 1976). Thus, the feedback mechanism, if it exists, may reduce the risk of swelling or lysis over the normal range of Na^+ entry and extrusion rates.

4. *Effect of aldosterone.* The mechanism by which aldosterone stimulates Na^+ transport in epithelia has been the object of much study (for reviews, *see* Edelman & Fimognari, 1968; Sharp & Leaf, 1973). In rabbit bladder, aldosterone increases G_t as well as I_{sc}, and pairs of (G_t, I_{sc}) values in aldosterone-stimulated bladder fall on the same curve as determined by effects of amiloride, Ca^{++}, Na^+-choline replacement, etc. (Lewis & Diamond, 1976, Fig. 16). The simplest interpretation is that aldosterone somehow stimulates amiloride-sensitive Na^+ channels in the apical membrane—e.g., by causing synthesis of more channels, by activating existing channels, or both. A second possible interpretation, if the postulated negative feedback from cell (Na^+) to apical G_{Na} does exist, is that

aldosterone might stimulate (or cause syntheses of) the Na^+ pump at the basolateral membrane, lowering cell (Na^+) and thereby increasing apical G_{Na} through the feedback mechanism. A third possible interpretation which also depends on feedback is that aldosterone might increase the energy supply to the pump, again lowering cell (Na^+) and increasing G_{Na}. Because of the evidence for the existance of feedback, our results do not discriminate among these interpretations, and a decision will be difficult.

5. *Rate-limiting step.* The rise in I_{sc} with increasing (Na^+) in the mucosal solution has not plateaued even at mucosal (Na^+) = 140 mM (Lewis & Diamond, 1976, Fig. 4). Similarly, the rise in I_{sc} when G_t and G_a are varied by agents thought to affect the apical membrane has not plateaued even at the highest G_t or G_a values attained in our experiments (Fig. 5 of this paper). This suggests that the pump in the basolateral membrane of rabbit bladder was not saturated under any of our experimental conditions, since an increase in apical Na conductance, presumably resulting in a rise in cell (Na^+), produced an increase in transepithelial Na flux. Had the pump been completely saturated and rate-limiting, a rise in apical conductance and in the cell (Na^+) could not have increased the pump rate and hence the transepithelial flux. Since increases or decreases in either the apical membrane conductance or the basolateral membrane pump actively result in changes in the steady-state transepithelial fluxes, neither membrane can be considered the sole rate-limiting step under our conditions.

Summary of model. Fig. 12 summarizes well-established findings as well as speculative interpretations about ion transport in rabbit urinary bladder. Most features of this model may apply qualitatively to other tight epithelia that transport Na^+, such as frog skin, toad bladder, and

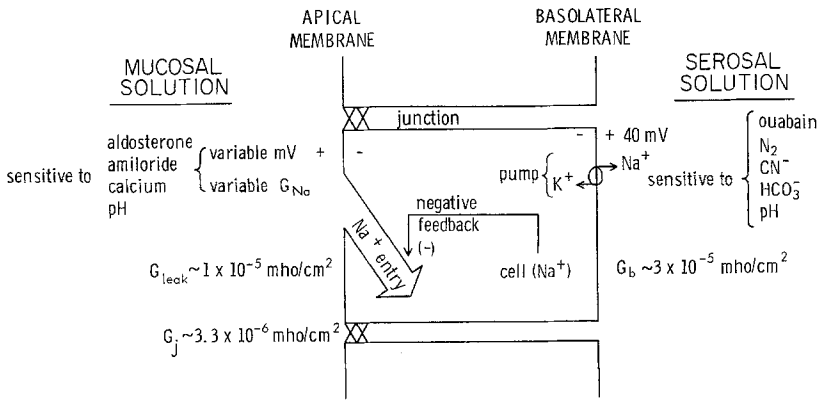

Fig. 12. Model of Na^+ transport mechanism in rabbit urinary bladder and other tight epithelia. *See text* for discussion

(except for higher junctional conductance) distal tubule and rabbit descending colon.

Junctional conductance is very low but may be increased by transepithelial voltages (and by osmotic gradients: DiBona & Civan, 1973; Bindslev, Tormey, Pietras & Wright, 1974).

The apical membrane contains a Na^+-entry channel that is stimulated by aldosterone and inhibited by amiloride or mucosal Ca^{++} or H^+. There is also a small leakage conductance to other ions (K^+, H^+, Cl^-?). ADH enhances apical conductance, but the effect is slight in rabbit urinary bladder, compared to some other epithelia.

Cell (Na^+) may exert negative feedback on apical G_{Na}.

The basolateral membrane contains a Na^+-K^+ exchange pump. We have no information about the Na^+/K^+ coupling ratio of this pump in rabbit bladder. The pump rate is increased by serosal HCO_3^- and decreased by N_2, cyanide and serosal ouabain or H^+, the effects of HCO_3^-, N_2 and cyanide probably being mediated by the energy supply rather than being direct effects on the pump. Passive Na^+ conductance of the basolateral membrane is very low, as evidenced by the very low Na^+ back-fluxes. The membrane has a leakage conductance to some other ion(s), possibly K^+. Either the basolateral or apical membrane, or both, has low G_{Cl}, as evidenced by the very low Cl^- fluxes. Consideration of resting potentials across these membranes in transporting bladders on open circuit, combined with likely ranges of intracellular ion concentrations, suggests that the main barrier to Cl^- is the apical membrane.

Still unresolved is the question what ion serves as a counterion for active Na^+ transport on open circuit, and whether this counterion or any other ion besides Na^+ has significant permeability in the amiloride-sensitive channel.

References

Bindslev, N., Tormey, J.McD., Pietras, R.J., Wright, E.M. 1974. Electrically and osmotically induced changes in permeability and structure of toad urinary bladder. *Biochim. Biophys. Acta* **332**:286

Bonting, S.L. 1970. Sodium-potassium activated adenosinetriphosphatase and cation transport. *In:* Membranes and Ion Transport. E.E. Bittar, editor. Vol. 1, p. 257. Wiley Interscience, London

Brown, K.M., Dennis, J.E., Jr. 1972. Derivative free analogues of the Levenberg-Marquardt and Gauss algorithms for nonlinear least squares approximation. *Numer. Math.* **18**:289

DiBona, D.R., Civan, M.M. 1973. Pathways for movement of ions and water across toad urinary bladder. 1. Anatomic site of transepithelial shunt pathways. *J. Membrane Biol.* **12**:101

Edelman, I.S., Fimognari, G.M. 1968. On the biochemical mechanism of action of aldosterone. *Recent Prog. Horm. Res.* **24**:1

Eisenberg, R.S., Johnson, E.A. 1970. Three-dimensional electrical field problems in physiology. *Prog. Biophys. Mol. Biol.* **20**:1

Fettiplace, R., Andrews, D.M., Haydon, D.A. 1971. The thickness, composition and structure of some lipid bilayers and natural membranes. *J. Membrane Biol.* **5**:277

Frömter, E. 1972. The route of passive ion movement through the epithelium of *Necturus* gallbladder. *J. Membrane Biol.* **8**:259

Frömter, E., Diamond, J.M. 1972. Route of passive ion permeation in epithelia. *Nature, New Biol.* **235**:9

Handler, J.S., Preston, A.S., Orloff, J. 1972. Effect of ADH, aldosterone, ouabain, and amiloride on toad bladder epithelial cells. *Am. J. Physiol.* **222**:1011

Higgins, J.T., Jr., Cesaro, L., Gebler, B., Frömter, E. 1975. Electrical properties of amphibian urinary bladder epithelia. 1. Inverse relationship between potential difference and resistance in tightly mounted preparations. *Pfluegers Arch.* **358**:41

Higgins, J.T., Frömter, E. 1974. Potential profile in *Necturus* urinary bladder. *Pfluegers Arch.* **347**:R32

Hviid Larsen, E. 1973. Effect of amiloride, cyanide and ouabain on the active transport pathway in the toad skin. Alfred Benzon Symposium V. N.A.Thorn and H.H. Ussing, editors. Munksgaard, Copenhagen

Koefoed-Johnsen, V., Ussing, H.H. 1958. The nature of the frog skin potential. *Acta Physiol. Scand.* **42**:298

Lewis, S.A., Clausen, C.J., Diamond, J.M. 1975. A transport-related conductance pathway in frog skin and urinary bladder. *Physiologist* **18**:291

Lewis, S.A., Diamond, J.M. 1976. Na^+ transport by rabbit urinary bladder, a tight epithelium. *J. Membrane Biol.* **28**:1

Lipton, P., Edelman, I.S. 1971. Effects of aldosterone and vasopressin on electrolytes of toad bladder epithelial cells. *Am. J. Physiol.* **221**:733

Loewenstein, W.R., Socolar, S.J., Higashino, S., Kanno, Y., Davidson, N. 1965. Intercellular communication: Renal, urinary bladder, sensory, and salivary gland cells. *Science* **149**:295

Macknight, A.D.C., Civan, M.M., Leaf, A. 1975*a*. The sodium transport pool in toad urinary bladder epithelial cells. *J. Membrane Biol.* **20**:365

Macknight, A.D.C., Civan, M.M., Leaf, A. 1975*b*. Some effects of ouabain on cellular ions and water in epithelial cells of toad urinary bladder. *J. Membrane Biol.* **20**:387

Reuss, L., Finn, A.L. 1974. Passive electrical properties of toad urinary bladder epithelium: Intercellular electrical coupling and transepithelial cellular and shunt conductances. *J. Gen. Physiol.* **64**:1

Sharp, G.W.G., Leaf, A. 1973. Effects of aldosterone and its mechanism of action on sodium transport. *In:* Handbook of Physiology. Section 8, Renal Physiology. R. W. Berliner and J. Orloff, editors. p. 815. American Physiological Society, Washington, D. C.

Shiba, H. 1971. Heaviside's "Bessel Cable" as an electrical model for flat simple epithelial cells with low resistive junctional membranes. *J. Theor. Biol.* **30**:59

Smith, P.G. 1971. The low-frequency electrical impedance of the isolated frog skin. *Acta Physiol. Scand.* **81**:355

Socolar, S.J., Politoff, A.L. 1971. Uncoupling cell junctions in a glandular epithelium by depolarizing current. *Science* **172**:492

Spenney, J.G., Shoemaker, R.L., Sachs, G. 1974. Microelectrode studies of fundic gastric mucosa: Cellular coupling and shunt conductance. *J. Membrane Biol.* **19**:105

Ussing, H.H., Erlij, D., Lassen, U. 1974. Transport pathways in biological membranes. *Annu. Rev. Physiol.* **36**:17

Walker, B.E. 1959. Radioautographic observations on regeneration of transitional epithelium. *Tex. Rep. Biol. Med.* **17**:375